Anisotropic exchange and superconductivity in UPt_3

M. R. Norman
Materials Science Division, Argonne National Laboratory, Argonne, Illinois 60439
(Received 26 June 1989; revised manuscript received 25 August 1989)

In this paper an anisotropic exchange interaction is derived and separately fit to high- and low-frequency magnetic neutron scattering data of UPt_3. This information is used to construct a superconducting pair potential in the strong spin-orbit coupling limit. Solutions of the gap equations show that both high- and low-frequency fluctuations support an A_{1u} order parameter, which differ in their vector orientation. Implications of these results in relation to the unique phase diagram UPt_3 will be discussed.

I. INTRODUCTION

Since the discovery of heavy-fermion superconductors (HFS), it has been speculated that magnetic fluctuations provide the pairing mechanism.[1] This speculation was based on similarities to ^{3}He. Both HFS and ^{3}He share the fact that they are almost magnetic (in fact, there is strong evidence that several HFS are weak magnets), and almost localized. Both of them also have nodes in their gap functions, indicated by non-s-wave pairing. The HFS case, though, is complicated by several facts: (1) the presence of a periodic lattice with more than one atom per unit cell, (2) a multisheeted Fermi surface composed of wave functions of differing radial/angular character, and (3) strong spin-orbit effects. This makes any theory for HFS more complicated to formulate than the analogous theory for ^{3}He.

Some steps, though, have been taken towards such a theory.[2-5] The basic idea is that the dynamic magnetic susceptibility, which enters as the spectral function in the self-energy equations (to be discussed in the following), is reasonably approximated by a function of momentum times a Lorentzian in frequency for HFS.[6] Thus the frequency and energy integrals can be performed separately, reducing the self-energy equation to a momentum integral over the Fermi surface.[3,5] In the normal state, this self-energy gives a mass renormalization proportional to the average susceptibility, and leads to a temperature dependence of the specific-heat coefficient in good agreement with experiment.[3] The self-energy in the superconducting state (gap equation), though, depends crucially on the momentum integral over the Fermi surface. Previous calculations[3,4,7,8] have used the results of earlier neutron scattering data,[6,9] which have an energy scale for magnetic fluctuations of the order of 5 meV with peaks in the susceptibility at $\mathbf{q}=(0,0,n)$ with n odd. These high-frequency fluctuations yield an odd-parity (A_{1u}) order parameter,[7] which will be further discussed in the following.

Recent neutron scattering data[10-12] indicate low-frequency fluctuations (with an energy scale of the order of 0.3 meV) that peak at $\mathbf{q}=(0.5,0,n)$ with n an integer. These fluctuations also have associated with them an elastic contribution, which corresponds to an ordered moment of about $0.02\mu_b$.[10] Doping leads to the same magnetic structure with a moment of about $0.7\mu_b$.[13] The data have now been normalized, and reveal that the peak value of the quasielastic contribution is a factor of three larger than the peak value of the (0,0,1) correlations discussed above,[11] so (0.5,0,0) correlations are of some importance.

In Sec. II, the magnetic fluctuation formalism will be reviewed, with a new anisotropic exchange version being developed and applied to high-frequency fluctuations in Sec. III and low-frequency fluctuations in Sec. IV. In Sec. V, strong-coupling corrections will be discussed, and finally in Sec. VI, the implications of these solutions vis-a-vis the phase diagram of UPt_3 will be commented on.

II. MAGNETIC FLUCTUATION FORMALISM

The magnetic fluctuation self-energy equations are developed in Refs. 3 and 7 (for related work, see Refs. 2, 4, 5, and 8). Basically, the real part of the normal self-energy gives a mass renormalization factor which is proportional to the momentum-averaged static susceptibility, and which decays in frequency away from the Fermi energy.[3] For purposes here, a BCS-type approximation is made where it is assumed that the effect of the normal self-energy is to replace the band structure density of states, N_0, by its renormalized value, N. If one assumes that the gap function is constant in frequency up to some cutoff, ω_c, one approximately obtains the following T_c equation:[3,7]

$$\Delta(\mathbf{k})=\ln(1.13\Gamma/T_c)\sum_{\mathbf{k}'} W(\mathbf{k}')V(\mathbf{k}-\mathbf{k}')\Delta(\mathbf{k}') \ . \quad (1)$$

$W(\mathbf{k}')$ is the density of states weighting over the Fermi surface, Γ is the neutron scattering linewidth, and V is the momentum-dependent part of the pair potential, to be derived below [note that the cutoff frequency, ω_c, does not appear in Eq. (1)]. The sum is done by taking the weights from a tetrahedral decomposition of the band structure Fermi surface which is in good agreement with deHaas-vanAlphen data for UPt_3, with the $\mathbf{k}$ mesh being defined as the center of mass of the tetrahedra.[7] In gen-

eral, $V(\mathbf{k}-\mathbf{k}')$ is not separable in $\mathbf{k}$ and $\mathbf{k}'$, but one can easily reduce the preceding equation to the following form for each irreducible group representation:

$$\sum_{\mathbf{k},\mathbf{k}'} M_{\mathbf{k}\mathbf{k}'}\Delta(\mathbf{k}')=0 \tag{2}$$

with $\mathbf{k}$ and $\mathbf{k}'$ now restricted to the irreducible wedge of the zone (for two-dimensional group representations, certain group operations cause a complex conjugation of the gap function, so the size of the matrix is twice that for the one-dimensional representations). T_c is then defined where the first eigenvalue of M crosses zero. For the case of UPt_3, a mesh of 137 $\mathbf{k}$ points in the irreducible wedge was used. Finally, the reader is referred to Sec. V for a discussion of frequency-dependent corrections to Eq. (1).

III. HIGH-FREQUENCY FLUCTUATIONS

The pair potential for (0,0,1)-type correlations will now be derived. The pair potential is usually assumed to be proportional to the dynamic susceptibility.[2-5] In this case, though, χ peaks at reciprocal lattice vectors in the q_z and q_x directions, reflecting antiferromagnetic correlations between the two U atoms in the UPt_3 unit cell. This function, therefore, is not lattice periodic, and thus when used in a gap equation, leads to gap functions which are not lattice periodic. One way to rectify this problem is to include Umklapp processes in the gap equation.[7,8] A better way to handle the problem, though, is to follow the same treatment used to fit the neutron scattering data in U_2Zn_{17}.[11,14] In this formalism, χ is treated as a 2×2 matrix, with the indices referring to the two sites in the unit cell. The standard random-phase-approximation (RPA) expression for χ is

$$\chi(\mathbf{q})=\chi_0/[1-I(\mathbf{q})\chi_0] , \tag{3}$$

where χ_0 is the bare ion susceptibility and $I(\mathbf{q})$ is the interaction function

$$I(\mathbf{q})=U+J\mathrm{Re}[\phi(\mathbf{q})] \tag{4a}$$

with U being the on-site repulsion, J an exchange interaction (negative for antiferromagnetic coupling), and $\phi(\mathbf{q})$ is $\sum_{\mathbf{R}} e^{i\mathbf{q}\cdot\mathbf{R}}$ with the sum being over nearest-neighbor vectors, $\mathbf{R}$,[4]

$$\phi(\mathbf{q})=\cos(q_z c/2)[\cos(q_x a/\sqrt{3})+2\cos(q_x a/2\sqrt{3})\cos(q_y a/2)+i\sin(q_x a/\sqrt{3})-2i\sin(q_x a/2\sqrt{3})\cos(q_y a 2)] . \tag{4b}$$

The generalization to the 2×2 matrix case involves replacing χ_0 by $\chi_0 1$ where 1 is the unit matrix, and $I(\mathbf{q})$ by

$$I(\mathbf{q})=\begin{bmatrix} U & J\phi \\ J\phi^* & U \end{bmatrix} . \tag{5}$$

Summing the same RPA series that yields Eq. (3), one obtains

$$\chi(\mathbf{q})=c\chi_0\begin{bmatrix} 1-U\chi_0 & J\chi_0\phi \\ J\chi_0\phi^* & 1-U\chi_0 \end{bmatrix} , \tag{6}$$

where

$$c^{-1}=(1-U\chi_0)^2-J^2\chi_0^2\phi\phi^* .$$

Similarly, the RPA equation for the pair potential

$$V(\mathbf{q})=I(\mathbf{q})+I(\mathbf{q})\chi_0 V(\mathbf{q}) \tag{7}$$

has the solution

$$V(\mathbf{q})=c\begin{bmatrix} U(1-U\chi_0)+J^2\chi_0\phi\phi^* & J\phi \\ J\phi^* & U(1-U\chi_0)+J^2\chi_0\phi\phi^* \end{bmatrix} , \tag{8}$$

where c is the same factor as in Eq. (6). Now what is measured for $\chi(\mathbf{q})$ is the sum of all four components of the matrix in Eq. (6), and for J negative this function peaks at (0,0,1). Note, though, that if one diagonalizes Eq. (8), the two eigenvalues are $V_\pm=V_{11}\pm|V_{12}|$, both of which are lattice periodic (see Ref. 15 for a related approach). The work of Refs. 7 and 8 essentially use a sum of these two eigenvalues as the pair potential. In general, the two eigenvalues should be used independently of one another (these are analogous to an optic and acoustic branch, respectively). In Fig. 1, $V_\pm$ are plotted for values of U and J that fit the neutron scattering data of Refs. 6

TABLE I. Coupling constants from high-frequency fluctuations (nearest-neighbor correlations). $V_\pm$ are the two eigenvalues of the pair potential, with $U=0.3$ and $J=-0.1$ in units of Γ (5 meV). The other coupling constants are less than 0.002. Note that the odd-parity solutions are orientated along the z axis.

	V_-		V_+
A_{1g}	0.049	A_{1u}	0.11
B_{2g}	0.0051	B_{2u}	0.055
E_{2g}	0.019	E_{2u}	0.019
E_{1g}	0.0076	E_{1u}	0.073

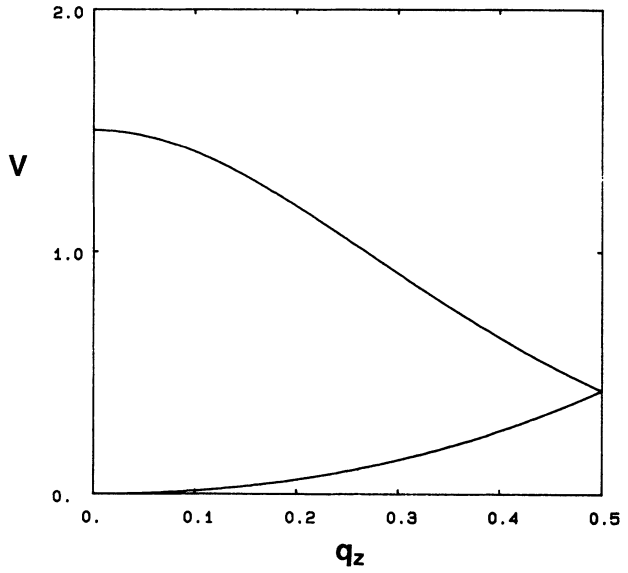

FIG. 1. Pair potential, V_{xx}, in units of Γ (5 meV) for high-frequency (nearest-neighbor) correlations plotted along the q_z direction, with $U=0.3$ and $J=-0.1$. The lower curve is the V_- eigenvalue, the upper one the V_+ eigenvalue. The potentials are similarly behaved along the q_x direction, except that there is a gap between the two at the zone boundary.

and 9 (see Table I). One sees that V_- will support even-parity solutions since it peaks at the zone boundary, whereas V_+ will support odd-parity solutions since it peaks at $q=0$.

The aforementioned has ignored spin effects. In a spin-only theory, V is multiplied by $\mathbf{s}\cdot\mathbf{s}$, where $\mathbf{s}$ is a spin vector. This results in a coefficient of $-\frac{3}{2}$ for even-parity states, and $\frac{1}{2}$ for odd-parity ones.[16] In UPt_3, there are strong spin-orbit effects, with the magnetic moments confined to the basal plane, and with χ_{zz} being about half of χ_{xx} and having none of the unusual temperature dependence that χ_{xx} has[17] (the latter arises from the antiferromagnetic correlations). This is taken into account by replacing $V\mathbf{s}\cdot\mathbf{s}$ with $V_{ii}s_is_i$, where i refers to spatial indices.[16] There is no evidence for basal plane anisotropy for the high-frequency fluctuations, so V_{yy} is set equal to V_{xx}, with the functional form given by either of the eigenvalues of Eq. (8). Since there are no AF correlations in χ_{zz},

$$V_{zz}=U/(1-0.5U\chi_0) \tag{9}$$

with the factor of 0.5 arising from the above-mentioned anisotropy. The inclusion of spin indices α, β, γ, and δ leads to the following gap equation (expressing $\mathbf{s}$ in Pauli matrix form):[18]

$$\Delta_{\alpha\beta}(\mathbf{k})=\ln(1.13\Gamma/T_c)\times\sum_{\mathbf{k}'}W(\mathbf{k}')V_{ii}(\mathbf{k}-\mathbf{k}')s^i_{\alpha\gamma}s^i_{\beta\delta}\Delta_{\gamma\delta}(\mathbf{k}')\ . \tag{10}$$

For even parity, this becomes ($\Delta=\Delta_{12}$)

$$\Delta(\mathbf{k})=-\ln(1.13\Gamma/T_c)\times\sum_{\mathbf{k}'}W(\mathbf{k}')[V_{xx}(\mathbf{k}-\mathbf{k}')+0.5V_{zz}]\Delta(\mathbf{k}')\ . \tag{11}$$

For odd parity, one expresses the gap matrix as $\Delta_{\alpha\beta}=i\mathbf{d}\cdot(\mathbf{s}s_y)_{\alpha\beta}$. V_{zz} drops out of the gap equation since it is a constant. Moreover, since $V_{xx}=V_{yy}$, only the d_z component survives

$$d_z(\mathbf{k})=\ln(1.13\Gamma/T_c)\sum_{\mathbf{k}'}W(\mathbf{k}')V_{xx}(\mathbf{k}-\mathbf{k}')d_z(\mathbf{k}')\ . \tag{11'}$$

For Eq. (11'), odd-parity basis functions in the strong spin-orbit coupling limit have to be used.[19] For instance, the A_{1u} basis function is of the form $k_z\hat{\mathbf{z}}$ (note that these functions are used only to define how the gap function transforms under group operations; the actual gap function is solved numerically on a grid in the irreducible wedge of the zone). In Table I, results are presented for solutions of Eqs. (11) and (11') with $U=0.3\Gamma$ and $J=-1.0\Gamma$ ($\chi_0\Gamma$ is about one for UPt_3). Tabulated is the coupling constant, λ, where λ^{-1} is equal to $N\Gamma\ln(1.13\Gamma/T_c)$ with $N\Gamma$ about three for UPt_3. The solution with maximal λ is A_{1u}, the same solution as that found in Ref. 7. This solution has a nodal line perpendicular to k_z for all sheets of the Fermi surface (the gap function vanishes not only for $k_z=0$ but also for $k_z=\pi/c$).

IV. LOW-FREQUENCY FLUCTUATIONS

Previous theoretical work using this formalism has ignored the low-frequency fluctuations which have an energy scale of order 0.3 meV. This was in spite of the fact that these fluctuations lead to an apparent ordered moment of 0.02 μ_b.[10–12,20] The reason they were ignored was because of their low-energy scale and the belief that the fluctuating part of the spectra was weaker than the high-frequency part, since the latter apparently saturate the observed static susceptibility.[6] Recently, it has been demonstrated that the peak value of the low-frequency spectra is a factor of three larger than the high-frequency peak value.[11] Therefore, they should be taken into consideration.

The first point to note is that the low-frequency data exhibit basal plane anisotropy.[11] In particular, the fluctuating moment is orientated along the resulting q vector. If one imagines turning the spins by 60° or 120° leaving the q vector fixed, the resulting configuration is not observed. This can be taken into account by allowing the exchange interaction to be anisotropic in the basal plane,[21] with the data being consistent with nearest-neighbor interactions in the plane. Since the nearest-neighbor distance in the plane is just a lattice constant, one does not need to use the 2×2 matrix formalism of Sec. III. The interaction of the form $J_{ii}s_is_i$ in Sec. III needs to be generalized to $J_{ij}s_iR_is_jR_j$ to explain the anisotropy, where R_i is the i'th component of the unit vector directed along the in-plane bonds. In the case considered here, there are four coefficients, J_{xx}, J_{yy}, J_{xy}, and J_{zz} (with J_{zz} set to zero as in the preceding section). Fourier transforming as before, one obtains for $I(\mathbf{q})$

$$I_{xx}=U+3J\cos(q_x\sqrt{3}a/2)\cos(q_y a/2)\ ,$$
$$I_{yy}=U+J[\cos(q_x\sqrt{3}a/2)\cos(q_y a/2)+2\cos(q_y a)]\ , \tag{12}$$
$$I_{xy}=-\sqrt{3}J\sin(q_x\sqrt{3}a/2)\sin(q_y a/2)\ .$$

Solving the RPA series for χ again, one obtains

$$\chi_{xx}=c\chi_0(1-\chi_0 I_{yy})\ ,$$
$$\chi_{yy}=c\chi_0(1-\chi_0 I_{xx})\ , \tag{13}$$
$$\chi_{xy}=c\chi_0^2 I_{xy}\ ,$$

where

$$c^{-1}=(1-\chi_0 I_y)(1-\chi_0 I_{xx})-\chi_0^2 I_{xy}^2\ .$$

For J negative, χ_{xx} has a peak at the wave vectors $\mathbf{q}=(0.5n,0,q_z)$ with n odd, as desired. If basal plane anisotropy is ignored, a maximum at $\mathbf{q}=(0.5,0)$ would not be possible. The peak would be at $\mathbf{q}=(0.5,0.5/\sqrt{3})$ instead. Note, though, that there is no q_z dependence in Eq. (12). The elastic neutron scattering data indicate that the peaks in χ happen at integer values of q_z. This can be enforced by multiplying J by a periodic function in q_z, which varies between zero and one, which we take to be $0.5+0.5\cos(q_z c)$ (there is no data on the q_z dependence for the quasielastic data, so this factor is somewhat arbitrary at this stage). A fit to the data of Refs. 11 and 12 indicates that $U=0.6$ and $J=-0.09$ in units of the high-frequency linewidth. Γ (the low-frequency linewidth of 0.3 meV will be referred to as Γ' in the following).

The analogous equation for the pair potential, V, is

$$V_{xx}/c=I_{xx}(1-\chi_0 I_{yy})+\chi_0 I_{xy}^2\ ,$$
$$V_{yy}/c=I_{yy}(1-\chi_0 I_{xx})+\chi_0 I_{xy}^2\ , \tag{14}$$
$$V_{xy}/c=I_{xy}\ ,$$

where c is the same factor as above, and V_{zz} is the same as Eq. (9) (with the above-mentioned different U of 0.6). V_{ij} is not invariant under hexagonal group operations, as the spin part has been left out at this stage. This is included by multiplying V_{ij} by $s_j s_j$. The gap equations for even parity and the d_z component of odd parity are the same as Eqs. (11) and (11'), except for the following replacement:

$$V_{xx}(\mathbf{k}-\mathbf{k}')\rightarrow 0.5[V_{xx}(\mathbf{k}-\mathbf{k}')+V_{yy}(\mathbf{k}-\mathbf{k}')]\ . \tag{15}$$

In Fig. 2, the potential $V_{xx}/2+V_{yy}/2$ is plotted from $\mathbf{q}=(0,0,0)$ to $\mathbf{q}=0.5,0,0)$. Since there is only one eigenvalue of the pair potential in this case, and that eigenvalue peaks at the zone boundary, it is expected that an even-parity solution will have maximal T_c.

In addition, independent odd-parity solutions are now allowed with d vectors in the basal plane because of the basal plane anisotropy in the pair potential. The coupled equations for the d_x and d_y components are

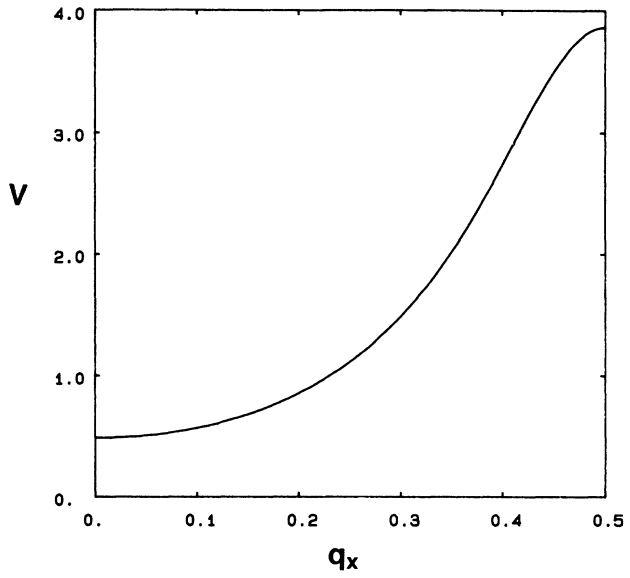

FIG. 2. Pair potential, $V_{xx}/2+V_{yy}/2$, in units of Γ (5 meV) for low-frequency (next-nearest-neighbor) correlations plotted along the q_x direction, with $U=0.6$ and $J=-0.09$. The absolute maximum in the potential is at $q=(0.5,0,0)$.

$$d_x(\mathbf{k})=\ln(1.13\Gamma'/T_c)\times\sum_{\mathbf{k}'}W(\mathbf{k}')[-V_1(\mathbf{k}-\mathbf{k}')d_x(\mathbf{k}')-V_{xy}d_y(\mathbf{k}')]\ ,$$
$$d_y(\mathbf{k})=\ln(1.13\Gamma'/T_c)\times\sum_{\mathbf{k}'}W(\mathbf{k}')[V_1(\mathbf{k}-\mathbf{k}')d_y(\mathbf{k}')-V_{xy}d_x(\mathbf{k}')]\ , \tag{16}$$

where

$$V_1=V_{xx}/2-V_{yy}/2\ .$$

Again, the basis functions can be found in Ref. 19. For instance, A_{1u} is of the form $k_x\hat{\mathbf{x}}+k_y\hat{\mathbf{y}}$.

In Table II, solutions for even and odd parity are shown (the definition of the coupling constant is the same as in the previous section, except that Γ in the logarithm is replaced by Γ'). The largest coupling constant is found for an A_{1u} solution with its vector orientated in the basal plane, although the A_{1g} coupling constant is only 20% lower. The A_{1u} solution has point nodes on all sheets of the Fermi surface (nodes not only for $k_x=0,k_y=0$ but also for $k_x=2\pi/\sqrt{3}a,k_y=0$; $k_x=0,k_y=4\pi/3a$, etc.). Although A_{1g} has the full symmetry of the hexagonal group, it has nodes because of the large value of U in the pair potential (in fact, the integral of the A_{1g} gap function over the Fermi surface is close to zero). The nodal structure, though, is rather complicated since it is not forced by symmetry. Calculations were also done where the periodic function in q_z multiplying J was squared [thus sharpening the peak at $\mathbf{q}=0.5,0,0)$ in the q_z direc-

TABLE II. Coupling constants from low-frequency fluctuations (next-nearest-neighbor correlations), with $U=0.6$ and $J=-0.09$ in units of Γ (5 meV). Note that the energy scale of these correlations is $\Gamma'=0.3$ meV. The notation z and x,y indicates the orientation of the odd-parity solutions.

			z	x,y
A_{1g}	0.20	A_{1u}	0.125	0.25
A_{2g}	0.0049	A_{2u}	0.0010	0.050
B_{1g}	0.0045	B_{1u}	0.0047	0.091
B_{2g}	0.062	B_{2u}	0.065	0.019
E_{2g}	0.12	E_{2u}	0.028	0.098
E_{1g}	0.089	E_{1u}	0.039	0.020

tion]. Both A_{1u} and A_{1g} coupling constants are reduced by 20%, but still are almost twice that for the other representations.

As for the gap functions, the A_{1u} solutions found for both high-frequency and low-frequency pairing are not consistent with current theoretical interpretations of the experimental data for UPt_3, which indicate an E_1 gap function. This will be discussed further in Sec. VI.

V. STRONG-COUPLING EFFECTS

The preceding treatment has ignored strong-coupling effects. In this formalism, the susceptibility is written as a function of momentum times a function of frequency, thus providing a clean separation between these two effects. In the following, only frequency-dependent effects are treated. These act to renormalize T_c, but do not change which group representation has the highest T_c. Momentum-dependent effects will be commented on at the end of the section.

The renormalization factor, Z, is given by the following equation:[3,22]

$$[1-Z(\omega)]\omega = cN_0\int_{-B}^{B}d\varepsilon\int_0^{\infty}d\Omega\langle \mathrm{Im}\chi(\mathbf{q},\omega)\rangle_{\mathbf{q}} \times[f(\varepsilon)/(\omega-\varepsilon+\Omega-i\delta) +f(-\varepsilon)/(\omega-\varepsilon-\Omega+i\delta)] , \quad (17)$$

where c is equal to $3U'^2/8\pi$ (where U' now defines the renormalization of χ relative to the band structure χ_b), N_0 is the bare (band-structure) density of states (assumed constant over the energy integral), $\langle\ \rangle_{\mathbf{q}}$ is a momentum averaging, and B is the bandwidth of the unrenormalized band structure (about 1000 K for UPt_3). Note that the Bose factors, $n(\Omega)$, have been dropped from the preceding expression since only low temperatures are of concern here. The dynamics susceptibility is approximated as[6]

$$\mathrm{Im}\chi(\mathbf{q},\omega)=\chi(\mathbf{q})\Gamma\omega/(\Gamma^2+\omega^2) \quad (18)$$

[with momentum averaging replacing $\chi(\mathbf{q})$ by χ_{av}]. For the real part of Z, the integral over $d\Omega$ becomes ($T=0$)

$$\Gamma^2/[(\omega-\varepsilon)^2+\Gamma^2][-\mathrm{sgn}(\varepsilon)\pi/2 -(\omega-\varepsilon)/\Gamma\ln|\Gamma/\omega-\varepsilon)|] . \quad (19)$$

The first term in the brackets can be analytically integrated over $d\varepsilon$, which yields the formula listed in Ref. 3 [$Z(0)=1+\pi cN_0\chi_{\mathrm{av}}$]. The second (small) term was missed previously (the author thanks Hartmut Monien for pointing this out), which is included by performing that part of the integral numerically. As discussed in Ref. 3, the value of c is about right to give the observed $Z(0)$ of 17 for UPt_3 (here, it is adjusted slightly to obtain exactly 17). The result for $\mathrm{Re}Z(\omega)$ is shown in Fig. 3 with an assumed bandwith of 15Γ. A curve similar to this was used in Ref. 3 to calculate the temperature dependence of the specific-heat coefficient in UPt_3 up to 20 K, which was found to be in good agreement with experimental data.

For the imaginary part, both $d\Omega$ and $d\varepsilon$ integrals can be done analytically, leading to the following expression ($T=0$):

$$\omega\mathrm{Im}Z(\omega)=cN_0\chi_{\mathrm{av}}(\pi\Gamma/2)\ln(1+\omega^2/\Gamma^2) . \quad (20)$$

This goes as ω^2 near the Fermi energy, just as it should for a Fermi liquid. This function is also plotted in Fig. 3.

The equation for the frequency-dependent gap function, $\Delta(\omega)$, is the same as Eq. (17), except that $d\varepsilon$ is replaced by[22]

$$c'/Z(\omega)d\varepsilon\int dS\,\mathrm{Re}\{\Delta(\mathbf{k},\varepsilon)/[\varepsilon^2-\Delta(\mathbf{k},\varepsilon)^2]^{1/2}\}\mathrm{sgn}(\varepsilon), \quad (21)$$

where dS is the surface element over the Fermi surface (normalized such that $\int dS=1$), and the constant c'

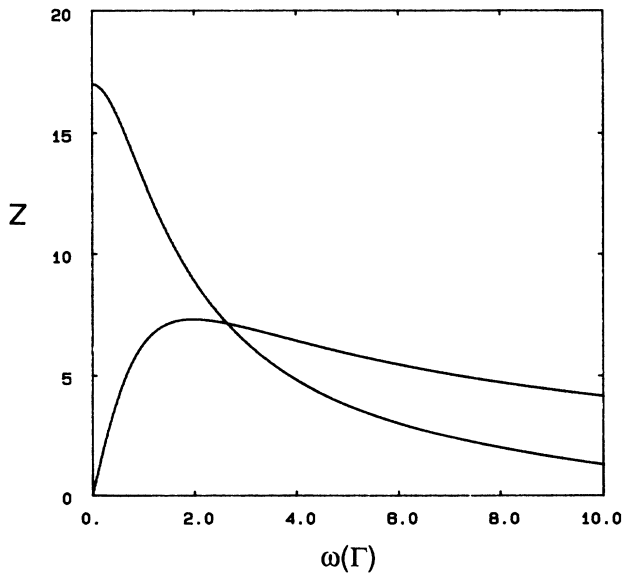

FIG. 3. Real (upper curve) and imaginary (lower curve) parts of the mass renormalization factor, Z, as a function of frequency in units of Γ (5 meV).

represents the momentum integral of the pair potential over $\mathbf{k}'$ [for simplicity's sake, it has been assumed here that the pair potential is separable in $\mathbf{k}$ and $\mathbf{k}'$, with $\Delta(\mathbf{k},\varepsilon)=\Delta(\varepsilon)f(\mathbf{k})$ and $V(\mathbf{k},\mathbf{k}')=Vf(\mathbf{k})f(\mathbf{k}')$]. For discussion purposes, the dS integral is performed analytically by assuming a Fermi sphere with $f(\mathbf{k})=\cos(\theta)$, where θ is the angle of $\mathbf{k}$ with respect to the k_z axis (this gap has a nodal line on the equator). As the $d\Omega$ integral is the same as before, only a numerical integral over $d\varepsilon$ has to be performed. $\Delta(\omega)$ is then solved interatively with c' adjusted each iteration so that $\Delta(0)$ is some set value (1 K for UPt_3), with the energy integral cutoff taken to be ten times the energy scale (Γ or Γ'). Only about five iterations are needed to converge the gap (the effect of Δ on Z is not taken into account, since such effects are small).

Results are shown in Figs. 4 and 5 for the two cases of pairing by high-frequency ($\Gamma=5$ meV) and low-frequency ($\Gamma=0.3$ meV) fluctuations, respectively, with Z calculated in both cases using the high-frequency Γ (this is consistent with the experimental specific-heat data, as shown in Ref. 3). Plotted are both the real and imaginary components of the gap function. For high-frequency pairing, Δ decays slowly in frequency (the more rapid decrease shown in Ref. 3 was due to neglect of the imaginary components of the self-energy), whereas for low-frequency pairing, Δ decays rapidly with frequency. This will lead to substantial strong-coupling corrections in the latter case, which will also act to reduce the T_c calculated in Sec. IV. Experimentally, there is some evidence for substantial strong-coupling corrections for UPt_3 from WHH-type fits to the upper critical field[23] from Ginzburg-Landau fits to the specific-heat data,[24] and so this would be in support of low-frequency pairing. Also,

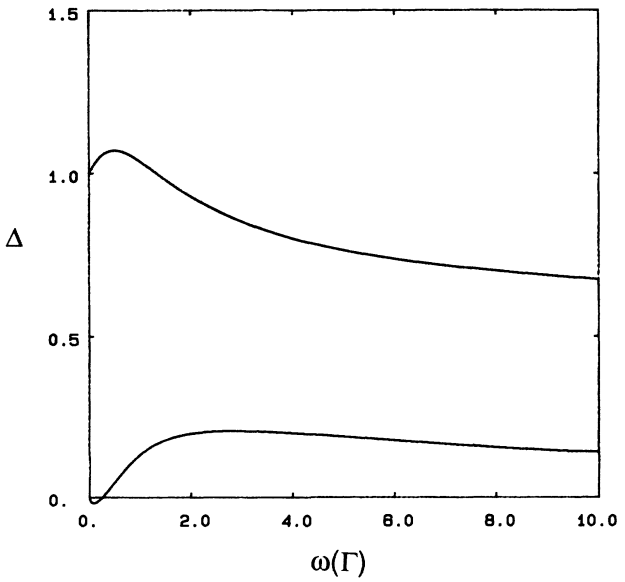

FIG. 4. Real (upper curve) and imaginary (lower curve) parts of the gap function, assuming high-frequency pairing, as a function of frequency in units of Γ (5 meV). The gap is normalized to one at zero frequency for plotting purposes (actually equal to 0.02 in these energy units).

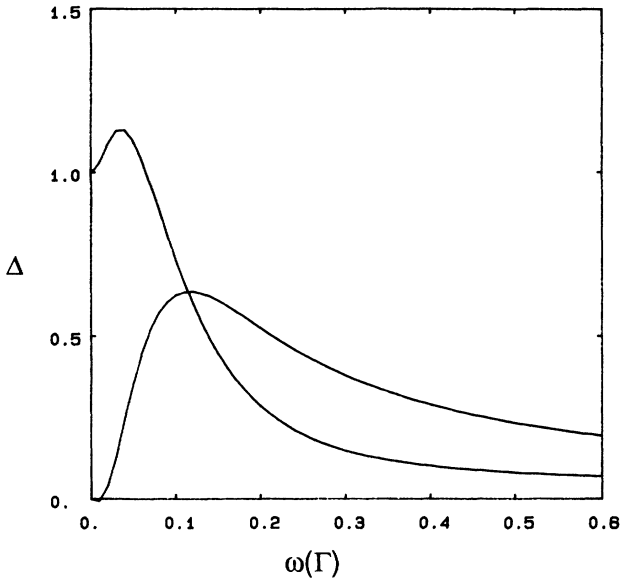

FIG. 5. Real (upper curve) and imaginary (lower curve) parts of the gap function, assuming low-frequency pairing, as a function of frequency in units of Γ (5 meV). Note that the low-frequency energy scale, Γ', is 0.06 in these units.

the slow frequency dependence of Δ for the high-frequency case appears quite unrealistic, as it implies pairing over a substantial frequency range of the order of 1000 K.

In ^{3}He, there are other strong-coupling effects due to the effect of gapping of the Fermi surface in the superconducting state on the pair potential[16] (this is responsible for stabilization of the A phase). In this current case, it is assumed that $\chi(\mathbf{q})$ is coming exclusively from local moment fluctuations (with quasiparticle interband terms being lumped into this definition), and thus this function should exhibit little change in the superconducting state. In fact, induced-moment form factor experiments see no change in $\chi(\mathbf{q})$ below T_c.[25] Moreover, there is no evidence for any change in the low-frequency quasielastic neutron scattering spectrum below T_c,[11] although neutron scattering experiments do indicate that the elastic part of the low-frequency fluctuations changes below T_c.[10-12] Finally, there is a recent claim of observing the quasiparticle (intraband) contribution to the dynamic susceptibility from low $\mathbf{q}$, low ω neutron scattering data.[26] Its predicted theoretical value is of the order of 20% of the bulk susceptibility,[27] and this term would be expected to change substantially in the superconducting state. The effect of this term on the pair potential is unknown at this time (it would be rather complicated to calculate).

VI. DISCUSSION

At this point, a discussion of the relevant experimental data on UPt_3 is in order. Specific-heat data show quite clearly that the specific-heat coefficient (C/T) varies linearly in the superconducting state,[28] indicating that the gap function has a nodal line. Moreover, transverse ultrasound data indicate that this nodal line is orientated perpendicular to the k_z axis.[29] Recently, it has been ob-

served that the specific-heat anomaly at T_c is actually two anomalies,[30] as predicted theoretically by Joynt.[31] This prediction was based on the fact that longitudinal ultrasound data exhibit an anomaly in magnetic field at about 0.6 H_{c2}, which indicates that the high-field superconducting state differs from the low-field one.[32] As originally pointed out by Volovik,[33] such an observation is consistent with the order parameter being from a two-dimensional group representation. As discussed by Joynt[31] and in greater detail by Hess *et al.*,[24] the weak magnetic ordering observed in UPt_3 has orthorhombic symmetry,[13] which would act to lift the degeneracy of the doubly-degenerate representation, thus leading to a splitting of the specific-heat anomaly at T_c. This requirement along with that of a nodal line would appear to restrict the order parameter to be from the E_1 representation, and the theoretical consequences of this have been worked out by a number of authors.[31,24,34] In particular, Hess *et al.*[24] have shown that such an order parameter can also account for the kinks seen in H_{c2} and they also predicted a kink in H_{c1} that has been recently observed.[35] As emphasized by Machida *et al.*,[34] the fact that Pt NMR shows no change in the Knight shift below T_c is supportive of an odd-parity state. This argument is not clearcut, though, since the quasiparticle contribution to χ is most likely small, although it should be emphasized that changes in the Knight shift of UBe_{13} have been observed below T_c by μSR data.[36] One problem with E_1 solutions is that they imply a spin or orbital moment along the c axis. Such an out-of-plane moment would appear to be inconsistent with what is known from neutron scattering data. Machida *et al.*[34] indicate that a splitting could also occur for a one-dimensional odd-parity state in the weak spin-orbit coupling limit.

This brings up the major question offered by this paper. Neither calculated gap function for high-frequency pairing or for low-frequency pairing is of E_1 symmetry. Moreover, although the high-frequency gap function has the required nodal lines, the author finds that solution physically unrealistic, since the observation of significant strong-coupling corrections[23,24] implies low-frequency pairing. Also, one's prejudices are that since the low-frequency fluctuations are the soft modes in the system, and actually lead to a weak magnetic instability, then they should play a dominant role in the pairing. The low-frequency gap function, though, has nodal points, which would not appear to be consistent with thermodynamic data though recent work measuring the London penetration depth does indicate an axial state.[37] Although the A_{1u} solution is a one-dimensional representation, it does have a vector orientation in the basal plane for low-frequency pairing. One could imagine that near T_c, the vector is actually rotated in a favorable direction in the basal plane by interaction with the weak magnetic moment. As the temperature decreased and the gap parameter increased, it would be energetically favorable to relax back to the unperturbed solution. This not only could cause a second transition (with accompanying kinks in H_{c2} and H_{c1}), but could in turn cause a decrease in the magnetic order parameter, as seen experimentally.[12]

Finally, it should be remembered that even at this stage, the construction of the pair potentials is rather primitive. First, an RPA approximation has been assumed with no momentum-dependent strong-coupling corrections. The latter are critical for determining the stable states of ^{3}He.[16] Currently, though, the experimental evidence favors little or no change in the dynamic susceptibility below T_c,[11] which would argue against strong feedback effects. Second, no matrix element effects have been included (i.e., the orbital and spin dependence of the quasiparticle wave functions have been ignored). Their inclusion could radically change the results of this paper, but the computational effort involved is substantially greater. The author is currently working on this problem, and hopes to report on it in a future paper. Certainly, it is clear from the neutron data that nearest-neighbor correlations are primarily responsible for the high-frequency fluctuations, whereas next-nearest-neighbor correlations are primarily responsible for the low-frequency ones. This, along with the observed basal plane anisotropy, puts certain constraints on the possible pair potentials. One missing piece of information at this stage is whether any nearest-neighbor correlations are involved in the low-frequency fluctuations. This matter could be investigated by obtaining quasielastic neutron scattering data for low-frequency fluctuations as a function of k_z (see note added in proof).

In conclusion, this work has used fits to both high- and low-frequency neutron scattering data to obtain model functions for the pair potential in the strong spin-orbit coupling limit. The result is that high-frequency pairing gives an A_{1u} gap function of the form $k_z\hat{\mathbf{z}}$, whereas low-frequency pairing gives an A_{1u} gap function of the form $k_x\hat{\mathbf{x}}+k_y\hat{\mathbf{y}}$. The latter solution is the most appealing on physical grounds. It remains to be seen, though, whether such a gap function can explain the unusual properties of UPt_3, or whether a more sophisticated theory is necessary to obtain order parameters of a differently symmetry, such as E_1.

Note added in proof. The q_z dependence of the pair potential for low-frequency fluctuations can be estimated by considering elastic scattering data at various reciprocal points.[13] The data indicate ferromagnetic coupling between near neighbors within the primitive cell (interplane), with the intensity being maximal at $(\frac{3}{2}, 0, 1)$. The resulting pair potential can be constructed using a combination of the functional forms given in Secs. III and IV. The new calculations predict an identical ordering of solutions as that in Table II, with the coupling constants increased by a factor of ~ 2.5 for even parity and ~ 3.5 for odd parity.

ACKNOWLEDGMENTS

The author would like to acknowledge helpful discussions with Collin Broholm, Bill Buyers, Lance deLong, Richard Klemm, Kathy Levin, Hartmut Monien, and Jim Sauls. This work was supported by the U.S. Department of Energy, Office of Basic Energy Sciences, under Contract No. W-31-109-ENG-38.

[1]P. W. Anderson, Phys. Rev. B **30**, 1549 (1984).
[2]K. Miyake, S. Schmitt-Rink, and C. M. Varma, Phys. Rev. B **34**, 6554 (1986).
[3]M. R. Norman, Phys. Rev. Lett. **59**, 232 (1987); Phys. Rev. B **37**, 4987 (1988).
[4]W. Putikka and R. Joynt, Phys. Rev. B **37**, 2372 (1988); **39**, 701 (1989).
[5]A. J. Millis, S. Sachdev, and C. M. Varma, Phys. Rev. B **37**, 4975 (1988).
[6]G. Aeppli, A. Goldman, G. Shirane, E. Bucher, and M.-Ch. Lux-Steiner, Phys. Rev. Lett. **58**, 808 (1987).
[7]M. R. Norman, Phys. Rev. B **39**, 7305 (1989).
[8]H. Monien and C. J. Pethick (unpublished).
[9]A. I. Goldman, G. Shirane, G. Aeppli, E. Bucher, and J. Hufnagl, Phys. Rev. B **36**, 8523 (1987).
[10]G. Aeppli, E. Bucher, C. Broholm, J. K. Kjems, J. Baumann, and J. Hufnagl, Phys. Rev. Lett. **60**, 615 (1988).
[11]C. Broholm, Ph.D. thesis, Riso National Laboratory, 1988.
[12]G. Aeppli, D. Bishop, C. Broholm, E. Bucher, K. Siemensmeyer, M. Steiner, and N. Stusser, Phys. Rev. Lett **63**, 676 (1989).
[13]A. I. Goldman, G. Shirane, G. Aeppli, B. Batlogg, and E. Bucher, Phys. Rev. B **34**, 6564 (1986).
[14]C. Broholm, J. K. Kjems, G. Aeppli, Z. Fisk, J. L. Smith, S. M. Shapiro, G. Shirane, and H. R. Ott, Phys. Rev. Lett. **58**, 917 (1987).
[15]R. Konno and K. Ueda, Phys. Rev. B **40**, 4329 (1989).
[16]W. F. Brinkman, J. W. Serene, and P. W. Anderson, Phys. Rev. A **10**, 2386 (1974); P. W. Anderson and W. F. Brinkman, in *The Physics of Liquid and Solid Helium,* Part 2, edited by K. H. Bennemann and J. B. Ketterson (Wiley, New York, 1978), p. 177.
[17]G. R. Stewart, Rev. Mod. Phys. **56**, 755 (1984).
[18]S. Nakajima, Prog. Theor. Phys. **50**, 1101 (1973).
[19]K. Ueda and T. M. Rice, Phys. Rev. B **31**, 7114 (1985); G. E. Volovik and L. P. Gor'kov, Zh. Eksp. Teor. Fiz. **88**, 1412 (1985) [Sov. Phys.—JETP **61**, 843 (1985)]; E. I. Blount, Phys. Rev. B **32**, 2935 (1935).
[20]P. H. Frings, Physica B **151**, 499 (1988).
[21]S. K. Sinha, G. H. Lander, S. M. Shapiro, and O. Vogt, Phys. Rev. B **23**, 4556 (1981); W. J. L. Buyers and T. M. Holden, in *Handbook on the Physics and Chemistry of the Actinides,* edited by A. J. Freeman and G. H. Lander (North-Holland, Amsterdam, 1985), Vol. 2, p. 239.
[22]N. F. Berk and J. R. Schrieffer, Phys. Rev. Lett. **17**, 433 (1966); D. J. Scalapino, in *Superconductivity,* edited by R. D. Parks (Marcel Dekker, New York, 1969), Vol. 1, p. 449.
[23]L. E. deLong, G. W. Crabtree, L. N. Hall, D. G. Hinks, W. K. Kwok, and S. K. Malik, Phys. Rev. B **39**, 7155 (1987).
[24]D. W. Hess, T. A. Tokuyasu, and J. A. Sauls, J. Phys. Cond. Matter **1**, 8135 (1989).
[25]C. Stassis, J. Arthur, C. F. Majkrzak, J. D. Axe, B. Batlogg, J. Remeika, Z. Fisk, J. L. Smith, and A. S. Edelstein, Phys. Rev. B **34**, 4382 (1986).
[26]G. Lonzarich (private communication).
[27]M. R. Norman, T. Oguchi, and A. J. Freeman, Phys. Rev. B **38**, 11 193 (1988).
[28]A. Sulpice, P. Gandit, J. Chaussey, J. Flouquet, D. Jaccard, P. Lejay, and J. L. Tholence, J. Low Temp. Phys. **62**, 39 (1986).
[29]B. S. Shivaram, Y. H. Jeong, T. F. Rosenbaum, and D. G. Hinks, Phys. Rev. Lett. **56**, 1078 (1986); P. Hirschfeld, D. Vollhardt, and P. Wolfe, Solid State Commun. **59**, 111 (1986).
[30]R. A. Fisher, S. Kim, B. F. Woodfield, N. E. Phillips, L. Taillefer, K. Hasselbach, J. Flouquet, A. L. Giorgi, and J. L. Smith, Phys. Rev. Lett. **62**, 1411 (1989); K. Hasselbach, L. Tailleer, and J. Flouquet, Phys. Rev. Lett. **63**, 93 (1989).
[31]R. Joynt, Superconductor Sci. Tech. **1**, 210 (1988).
[32]A. Schenstrom, M.-F. Xu, Y. Hong, D. Bein, M. Levy, B. K. Sarma, S. Adenwalla, Z. Zhao, T. Tokuyasu, D. W. Hess, J. B. Ketterson, J. A. Sauls, and D. G. Hinks, Phys. Rev. Lett. **62**, 332 (1989).
[33]G. E. Volovik, J. Phys. C **21**, L221 (1988).
[34]K. Machida, M. Ozaki, and T. Ohmi, (unpublished).
[35]B. S. Shivaram, J. J. Gannon, Jr., and D. G. Hinks, Phys. Rev. Lett. **63**, 1723 (1989).
[36]R. H. Heffner, D. W. Cooke, A. L. Giorgi, R. L. Hutson, M. E. Schillaci, H. D. Rempp, J. L. Smith, J. O. Willis, D. E. MacLaughlin, C. Boekema, R. L. Lichti, J. Oostens, and A. B. Denison, Phys. Rev. B **39**, 11 345 (1989).
[37]B. S. Shivaram, J. J. Gannon, Jr., and D. G. Hinks (unpublished).